Supporting Information

Spitschan et al. 10.1073/pnas.1400942111

SI Methods

Overview. To quantify the contributions of different photoreceptors to the pupillary control system and characterize its temporal properties, photoreceptor-directed light stimuli were delivered using the method of silent substitution while the consensual PLR was measured. The PLR was probed with spectral modulations directed toward L+M cones, melanopsin, and S cones. An isochromatic modulation that stimulated all photoreceptors with equal contrast and phase was also used.

Observers. A total of 16 observers (age 23 ± 6 y; nine male, seven female) took part in the experiments. All had corrected visual acuity of 20/30 or better and normal color vision as assessed with Ishihara plates (1). Two of these observers (subjects 01 and 02, both male, ages 43 and 23 y, and both authors of this paper: G.K.A. and S.J.) took part in extensive measurements. Four other observers were recruited for the study but excluded from the protocol because of poor eye tracking owing to epicanthal folds or an inability to suppress blinking. The study was approved by the University of Pennsylvania Institutional Review Board, and all subjects provided written informed consent.

Visual Stimuli. Visual stimuli were presented using a custom apparatus that allowed modulation of the spectral content of the light reaching the eye. This was achieved with a digital light integrator (OneLight VISX Spectra Digital Light Engine), which produces arbitrary spectral power distributions within the visible wavelengths. The digital light integrator device works as follows. Light from a xenon arc lamp is collimated and passed through a diffraction grating to spatially separate individual wavelengths. Each wavelength is then imaged on individual columns of a digital light processing (DLP) chip (768 rows by 1,024 columns). Each row in a column on the chip can be turned on or off, controlling the emitted power at each wavelength, and thus allowing for the construction of arbitrary spectral power distributions. Rather than individually addressing the 1,024 columns of the DLP, chip columns were grouped in bands of eight, yielding a device space with 128 effective monochromatic primaries with a peak spectral power between 414 and 780 nm, spanning the visible spectrum (mean full width at half maximum of 16 ± 0.6 nm). For the control data presented in Figs. S4 and S5, which were collected some months after the main experiments, chip columns were instead grouped in bands of 16 and some of the other parameters provided below (background luminance and chromaticity) also differed slightly from those used in the main experiments.

Stimulus modulations were constructed to selectively stimulate specific classes of photoreceptors (see Dataset S1 for a tabulation of the spectra used), as described below. The contrast of each modulation followed a sinusoidal temporal profile (200 discrete steps), alternating between maximum positive and negative contrast in photoreceptor contrast space around a neutral background (the origin of the photoreceptor contrast space), which was defined as ∼50% of the maximal intensity of the device primaries (CIE 1931 *xy* chromaticity, mean ±1 SD across experimental sessions: $x = 0.398 \pm 0.01$, $y = 0.433 \pm 0.002$). In a typical experiment, the stimuli were modulated around a background well above rod-saturating levels (2) (background light level varied somewhat as the lamp in the device aged; mean value across sessions 802 cd/m^2; range across sessions 382–1,033 cd/m^2). Stimuli were modulated at 0.01, 0.05, 0.1, 0.5, 1, and 2 Hz for subjects 01 and 02. Subjects 03–16 were studied only at 0.05 and 0.5 Hz.

Four primary directions in photoreceptor contrast were probed: melanopsin-directed, S-cone-directed, L+M (stimulating L and M cones with equal contrast), and isochromatic (equal contrast stimulation of cones and melanopsin). Two variants of the S-directed modulation were used, as described below. All modulations produced ∼50% predicted contrast on their targeted photoreceptors.

We tested the effect of background luminance on pupil responses by placing neutral density filters with known spectral transmissivity in the optical path (Fig. S1). We also examined, in subjects 01 and 02, whether the complex sum of the individual photoreceptor-directed modulations (S+M+L+melanopsin) resembled the response to isochromatic modulations (Fig. S8). This was the case to good approximation, and the isochromatic response across temporal frequencies resembled previously published data (Fig. S9). Although broad-band, the isochromatic modulation was not simply a scaling of the background spectrum; it was constructed to produce equal predicted contrast on all photoreceptor classes (cones and melanopsin).

Silent Substitution. The method of "silent substitution" was used to direct visual stimuli to specific photoreceptors or sets of photoreceptors (3–5). Silent substitution stimuli were produced by minimizing an error function over modulation of the device primaries that quantified the quadratic loss between the desired contrast across targeted photoreceptor classes and the photoreceptor contrasts computed from predicted spectra given the device primary modulations (6), subject to the constraint that the predicted contrast for the to-be-silenced photoreceptors was zero. MATLAB's fmincon routine was used to perform the constrained optimization.

Because the number of device primaries exceeded the number of photoreceptor classes, the optimization was additionally constrained by enforcing smoothness on the predicted modulation spectral power distributions. Modulations were also required to avoid the extrema of the device gamut.

The tabulated 10° Stockman–Sharpe/CIE cone fundamentals were used as estimates of LMS-cone spectral sensitivities (7, 8). Spectral sensitivity of the melanopsin photopigment was estimated by shifting the Stockman–Sharpe nomogram (8) to have peak spectral sensitivity at $\lambda_{max} = 480$ nm in accordance with previous reports of melanopsin peak spectral sensitivity (9, 10). Prereceptoral filtering was assumed to match that of cones. Melanopsin peak optical density was taken as 0.3, within the range of values (between 0.1 and 0.5) used in other recent pupillometric and psychophysical studies of melanopsin response in human (5, 6, 11) but higher than values suggested by neurophysiology (9, 12). The spectral sensitivities of the photoreceptors are shown in Fig. 1*A*.

Checks on Photoreceptor Isolation. The degree to which isolation of specific classes of photoreceptors is achieved by a nominally isolating modulation depends on both certainty regarding the spectral sensitivities of the photoreceptors in question and the quality of the spectral characterization of the digital light integrator.

Uncertainty in photoreceptor sensitivity is produced by individual variation as well as with variation in effective photoreceptor sensitivity across the retina. The CIE standard for cone fundamentals (7) has parameters to account for field size, pupil size, and observer age. These in turn control physiological parameters such as lens and macular pigment density. We explored how much contrast the "standard" S-directed modulation, computed as described above, produced for melanopsin. To do so, we

computed the contrast seen by melanopsin photoreceptors as we varied estimates of their spectral sensitivity as illustrated in Fig. S2 *A* and *B*. The left-hand plots in Fig. S2*C* show the results for the modulations predicted by our device characterization. Melanopsin contrast is zero for the targeted melanopsin spectral sensitivity (Fig. S2*C*, *Upper Left*). There is, however, modest contrast "splatter" onto melanopsin when wavelength of peak spectral sensitivity (λ_{max}) and the CIE standard age parameter (which affects primarily lens density) are varied. Repeating the same explorations but with direct measurements of the modulating spectra at maximal and minimal contrast levels revealed somewhat larger splatter than obtained with respect to the predicted spectra (Fig. S2*C*, *Upper Right*). The differences between predicted and measured spectra presumably reflect drifts in the digital light integrator between calibration and validation measurement, as well as deviations between the performance of the light integrator and that of an ideal device. Similar splatter plots are obtained if instead we use a physiologically based estimate of melanopsin spectral sensitivity (Fig. S2*C*, *Lower*).

Although the contrast splatter for the S-directed stimulus onto melanopsin was modest compared with the ∼50% modulation produced in the S cones, for some parameter choices it was negative. This raised the possibility that the measured out-of-phase S response arises not from S-cone signals but from out-of-phase contrast splatter from our S-directed stimulus onto the melanopsin photoreceptors. To eliminate this possibility, we computed an "alternative" S-cone modulation. This modulation was constructed using the silent substitution procedure as described above, but with an increased number of photoreceptor sensitivities that were silenced. In particular, we silenced not only the L cones, M cones, and standard melanopsin photoreceptors, but also the rods and a variant of melanopsin with its λ_{max} value shifted to 495 nm. Rod spectral sensitivity was estimated by taking λ_{max} = 500 nm and peak optical density as 0.333, within the range of previous estimates (13, 14). The alternative S modulation reduces the contrast splatter onto melanopsin for the predicted spectra (Fig. S2*D*, *Left*) but increases it for the measured spectra (Fig. S2*D*, *Right*). Importantly, however, the contrast splatter for the measured spectra was positive for all melanopsin parameters and thus there is little chance of an out-of-phase melanopsin-based response for this modulation. The alternative S splatter onto L and M cones was small and also positive. The "standard" modulation was used for subjects 01 and 02. A direct empirical comparison for these subjects indicates that their response to the standard and alternative S-directed modulations was not different (Fig. S3). For subjects 03–16 the alternative S-directed modulation was used.

To calculate splatter in a biologically plausible range of age of λ_{max} parameter values, we estimated the variability in these parameters as follows. For the estimates in λ_{max}, we assumed SDs of 1.5, 0.9, and 0.8 nm about their nominal λ_{max} for L, M, and S cones (15). For melanopsin, we assumed an SD of 1.5 nm, conservatively corresponding to the largest SD across the cone classes. To estimate variability in lens density, we extracted the SD of the vertical measurement residuals of predicted vs. chronological age from a two-component lens density model (16). We found that the SD of the predicted age parameter for lens density owing to individual variability is 7 y. Using these estimates, we derived 95% and 99% confidence regions (± 2 and ± 3 SDs), assuming independence between λ_{max} and age, and obtained the minimum and maximum splatter values in these ellipses (Fig. S2). For the main modulations, we determined these confidence ellipses using a 2D Gaussian with mean age of 21 y (mean age of all subjects excluding subject 01), and an SD of 7 y, and the nominal λ_{max} specific to each cone class and its SD given above. In the same fashion, we furthermore determined the confidence ellipses for subject 01 only using the observer's age (43 y) and the same age variability as well as λ_{max} and calculated splatter within these ellipses for both the main modulations and the supplementary control modulations (Figs. S4 and S5). To obtain an estimate of the expected value for absolute splatter, we used the same 2D Gaussians and calculated expectation. Table S1 provides the resulting values for contrast splatter for each of our main stimulus modulations onto each photoreceptor class, computed in this way. The legend of Fig. S5 provides the key values for the supplementary control modulations. In all of these calculations we assumed that L, M, and S cones underwent self-screening according to a percentage of pigment bleached corresponding to the background spectrum with a photopic luminance of 800 cd/m^2 seen through our 4.7-mm-diameter artificial pupil (discussed below), corresponding approximately to the mean light level across sessions. This corresponded to percentage pigment bleached of 44.37, 37.03, and 3.25% for L, M, and S cones, respectively.

Across observer age and nominal λ_{max}, both S-directed modulations produce very little splatter onto the L and M cones, making it unlikely that our measured S responses are artifactually mediated by L or M cones. The expected absolute value of the contrast splatter of our L+M-directed modulation onto S and melanopsin is generally small (3.34 and 1.3%, respectively, for the younger observers and melanopsin-a spectral sensitivity estimate; see Table S1 for other variants of the calculations), but for some spectral sensitivity estimates does approach 10%. Note, however, that if our L+M response was mediated primarily by an artifactual S or melanopsin response, we would expect the S or melanopsin responses to be larger than the L+M response at all temporal frequencies. This is not the case (Figs. 3 and 4). Similarly, the expected absolute value of contrast splatter of our melanopsin modulation onto L, M, and S cones is also small (4.63, 3.43, and 8.2%, respectively). There can, however, be as much as ∼10% splatter onto the M cones and ∼13% splatter onto the S cones for some spectral sensitivity estimates, with the sign of such splatter being negative in some cases. Again, the possibility that our melanopsin response might be cone-mediated is ruled out by the fact that if our melanopsin response were mediated by splatter onto cones we would expect the L+M or S-cone response to exceed the melanopsin response at all temporal frequencies. This is clearly not the case for subject 02 (Fig. 4) and not the case for S-cone responses for subject 02 (Fig. 4, low temporal frequencies). With respect to the S-cone case, the average melanopsin response of subjects 01–16 also clearly exceeds their average S-cone response at 0.05 Hz (Fig. 5*A*). In addition, the shape of the temporal transfer function (TTF) between melanopsin and L+M differs markedly for both subjects 01 and 02, also speaking against the possibility that the melanopsin response is mediated by L+M splatter. Further evidence that the melanopsin response is not mediated by splatter onto L+M cones is provided by the control data for subject 01 presented in Figs. S4 and S5.

Stimulus Display. Light from the digital spectral integrator is collected and passed out of the device through a fiber optic cable (FTIIG16860-40, total length 40 feet; Fiberoptics Technology, Inc.) to a custom-made eyepiece. Within the eyepiece, light first passed through a lens (12-mm diameter, −18-mm focal length), diffusing the light and back-projecting it onto an opal diffusing glass (35-mm diameter). Located on the front surface of the diffusing glass was a Plexiglas disk (5.5-mm thickness, 35-mm diameter), which had a reticular etched surface pattern. The central 5° of visual angle (2.18-mm diameter) was blackened and the etched vertical, horizontal, and two annular grid markers were visible. The observer was instructed to fixate the center of the blackened central disk.

The observer viewed the diffusing glass through an additional lens (25-mm diameter, 25-mm focal length) that could be adjusted to bring the diffuser into focus. A rubber eye cup was affixed to the

viewing end of the eyepiece and held in place a black, opaque plastic disk with a 4.7-mm central aperture. The observer viewed the stimulus using his or her dilated eye through this artificial pupil to equate retinal irradiance across subjects. Dilation was achieved with 0.5% proparacaine hydrochloride as a local anesthetic followed by 1% tropicamide. Throughout the experiment artificial tears were applied if needed. An adjustable chin and forehead rest was used to position the head of the observer in the rig.

Stimulus Calibration. The light exitant from the eyepiece was characterized using a spectroradiometer (PR-670 SpectraScan; Photo Research, Inc.), which imaged the eyepiece diffuser through the eyepiece lens. The power at each wavelength was measured for each of the 128 primaries individually to allow a forward characterization of the device. To characterize nonlinearities between settings of the device primaries and the exitant light, measurements were taken at 16 device primary intensity levels for three of the 128 effective primaries. These "gamma functions" were of similar shape and were averaged and linearly interpolated to produce an overall function for linearization of each primary. The additivity of a subset of effective primaries was verified to hold to good approximation. Finally, measurements were taken of dark response (i.e., when all primaries are turned off). Following the production of device primary settings that produced the specified desired contrasts on the photoreceptors with respect to the background, these modulations were validated with spectroradiometric measurements.

Pupillometry. Pupil diameter at the nonstimulated eye was measured using an infrared red video pupillometry system (Video Eye Tracker; Cambridge Research Systems Ltd.). The diameter was polled at a frequency of 50 Hz, with a few dropped measurements. Absolute size was calibrated before the experiments using a supplied calibration scale. The pupil detection algorithm supplied by the eye tracker was used; data traces were recorded for offline processing.

Raw data traces were smoothed and resampled using a seventh-order polynomial Savitzky–Golay filter. Missed samples owing to polling delay, blinks, or eye movements were identified, as were "spikes" (data point windows in which the signal changed by 20% overall, or in which the signal changed by more than 2 SD of the signal in the entire time series). Trials with more than 20% of samples being thus identified as "bad" were discarded entirely. The first 20 or 5 s (for the 120- and 45-s trials, respectively) of each trial were discarded before fitting to allow measurement of the amplitude and phase response with the pupil in a steady state. Mean pupil diameter was not found to be different across modulation directions and frequencies (Fig. S7). For this reason, the pupillary response was quantified as proportion change from baseline.

To characterize the pupillary control system, amplitude and phase of the pupillary response were obtained by performing least-squares spectral fitting: Sine and cosine waves were fit to obtain amplitude and phase of the pupillary response at the stimulus frequency (fundamental) and the second harmonic. The primary analyses in this paper are of the response at the fundamental.

The SEM of the pupillary response across trials was estimated by a boot-strap procedure. Trials were randomly sampled with replacement up to the total number of trials and the average response across this sampling was obtained. The SD of the bootstrapped averages was taken as the SEM response.

Procedure. For subjects 01 and 02, data were collected in blocks of 36 120-s trials. Each block consisted of six trials at each of the six temporal frequencies, all of a single photoreceptor-directed modulation. Both subjects completed two blocks each of the four photoreceptor directions (L+M, Mel, "standard" S, and isochromatic). Subject 02 completed an additional block of 27 trials of each photoreceptor direction that contained only the three lowest frequencies of modulation to address the greater measurement noise present at lower temporal frequencies. All blocks used a different, counterbalanced ordering of stimuli. Each block began with 5 min of adaptation to the background, and the static background was presented between each trial. The subject pressed a button to initiate each trial. After confirming the quality of the eye-tracking signal, the modulation was presented, windowed at onset by a 3-s half-cosine. All measurements were obtained in a darkened room.

For subjects 03–16, data were collected in blocks of 27 45-s trials. Each block consisted of nine trials of each of the photoreceptor-directed modulations (L+M, Mel, and "alternative" S), all at a single temporal frequency. Each subject completed four blocks at 0.05-Hz stimulation and two blocks at 0.5 Hz. All blocks used a different, counterbalanced ordering of the stimuli. Additionally, the phase of stimulus onset was randomized across trials in units of $\pi/8$ to remove possible anticipatory pupil responses to trial onset. Stimulus phase randomization was accounted for in the data analysis procedures so that data were aggregated with respect to a common stimulus phase.

Model. The amplitude and phase of pupillary response for two subjects (sub01 and sub02) were fit with a two-filter model of temporal sensitivity (17). For both the fast and slow filters, the model implements an impulse response of the form

$$h(t) = u(t)\left[\tau(n-1)!\right]^{(-1)}(t/\tau)^{(n-1)}e^{(-t/\tau)},$$

where $u(t)$ is the unit step function, n the order (number of stages) of the filter, and τ a time constant. For such a filter, the amplitude and phase as a function of temporal frequency are (17)

$$\left|H(\omega)\right| = (i2\pi\omega\tau + 1)^{-n/2}$$

and

$$\angle H(\omega) = -n\tan^{-1}(2\pi\omega\tau) - 2\pi\omega t_0.$$

The pupil response is described by a difference of the fast and slow responses, where the fast and slow filters have independent time constants (τ_1, τ_2) and amplitudes (k_1, k_2). The two filters could be synergistic (opposite sign for k_1 and k_2) or opponent (same sign for k_1 and k_2). We used a first-order filter ($n_1 = 1$) for the fast component and a fourth order for the slow component, with these values chosen via examination of the fit quality obtained with various choices of filter order.

Amplitude and phase of the pupil responses across stimulation frequency were fit jointly for each modulation direction. The error function weighted the amplitude and phase residuals by the SEM of each. Best-fitting parameters were found using constrained minimization. A common time delay was fixed for each observer independently (250 ms for sub01; 230 ms for sub02) and kept constant across modulation directions. These values are consistent with the pupillary response latencies observed for the ages of our subjects (18). The linear phase effect corresponding to the delay was incorporated into the model predictions.

The group average data (subjects 01–16) were fit using the same model. Initial fit parameters were derived from those obtained for subject 01. For both the fast and slow components of the filter, time constants were fixed and the time delay was set to 250 ms. The amplitude parameters were then fit to minimize quadratic loss between observed and model amplitude and phase. Because the fits to the data are underconstrained owing to experimental sampling at only two frequencies (0.05 and 0.5 Hz), allowing changes only in the amplitude parameters provides an adequate compromise between overfitting and preserving the shape of the temporal transfer functions obtained from the extensively studied subjects. The parameters for subject 01 were used because the data from this subject are more representative of the group data than those of subject 02.

1. Ishihara S (1977) *Tests for Colour Blindness* (Kanehara Shuppen Company, Tokyo).
2. Aguilar M, Stiles WS (1954) Saturation of the rod mechanism of the retina at high levels of stimulation. *Opt Acta (Lond)* 1:59–65.
3. Donner KO, Rushton WA (1959) Retinal stimulation by light substitution. *J Physiol* 149:288–302.
4. Estévez O, Spekreijse H (1982) The "silent substitution" method in visual research. *Vision Res* 22(6):681–691.
5. Tsujimura S, Ukai K, Ohama D, Nuruki A, Yunokuchi K (2010) Contribution of human melanopsin retinal ganglion cells to steady-state pupil responses. *Proc Biol Sci* 277(1693):2485–2492.
6. Viénot F, Brettel H, Dang TV, Le Rohellec J (2012) Domain of metamers exciting intrinsically photosensitive retinal ganglion cells (ipRGCs) and rods. *J Opt Soc Am A Opt Image Sci Vis* 29(2):A366–A376.
7. CIE (2006) Fundamental chromaticity diagram with physiological axes – Part 1. Technical Report 170-1 (Central Bureau of the Commission Internationale de l'Éclairage, Vienna).
8. Stockman A, Sharpe LT (2000) The spectral sensitivities of the middle- and long-wavelength-sensitive cones derived from measurements in observers of known genotype. *Vision Res* 40(13):1711–1737.
9. Brown TM, et al. (2013) The melanopic sensitivity function accounts for melanopsin-driven responses in mice under diverse lighting conditions. *PLoS ONE* 8(1):e53583.
10. Enezi Ja, et al. (2011) A "melanopic" spectral efficiency function predicts the sensitivity of melanopsin photoreceptors to polychromatic lights. *J Biol Rhythms* 26(4): 314–323.
11. Horiguchi H, Winawer J, Dougherty RF, Wandell BA (2013) Human trichromacy revisited. *Proc Natl Acad Sci USA* 110(3):E260–E269.
12. Do MT, et al. (2009) Photon capture and signalling by melanopsin retinal ganglion cells. *Nature* 457(7227):281–287.
13. Alpern M, Pugh EN, Jr (1974) The density and photosensitivity of human rhodopsin in the living retina. *J Physiol* 237(2):341–370.
14. Zwas F, Alpern M (1976) The density of human rhodopsin in the rods. *Vision Res* 16(2): 121–127.
15. Webster MA, MacLeod DI (1988) Factors underlying individual differences in the color matches of normal observers. *J Opt Soc Am A* 5(10):1722–1735.
16. Xu J, Pokorny J, Smith VC (1997) Optical density of the human lens. *J Opt Soc Am A Opt Image Sci Vis* 14(5):953–960.
17. Watson AB (1986) Temporal sensitivity. *Handbook of Perception and Human Performance*, eds Boff K, Kaufman L, Thomas J (Wiley, New York), Vol 1, pp 6-1–6-43.
18. Loewenfeld IE, Lowenstein O (1993) *The Pupil: Anatomy, Physiology, and Clinical Applications* (Iowa State Univ Press, Ames, IA), 1st Ed.

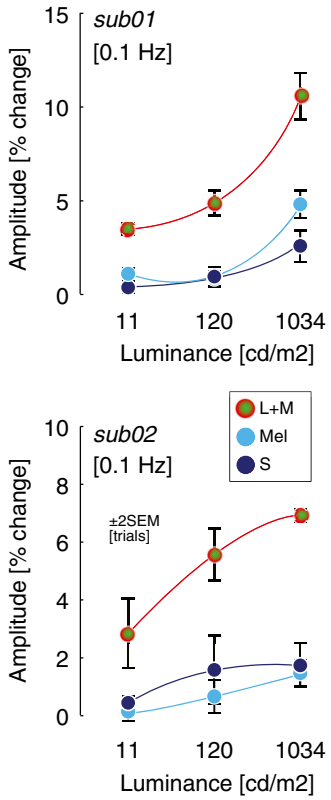

Fig. S1. Pupil response to L+M-, melanopsin-, and S-directed modulation scales with background light level. Pupil response to 0.1-Hz modulation as a function of background light level. Each panel shows the results for one subject and three photoreceptor targeted modulations. If rod signals were playing a substantial role in the response at the highest background luminance, that contribution would be expected to increase as the background light level dropped. Although such an increase could be balanced by a concomitant decrease in cone or melanopsin contribution to the responses, these data speak against the possibility that rod signals—which might arise through stimulation by scattered light onto relatively dark adapted rods outside of area of the stimulus—are contributing to the pupil response studied in this paper.

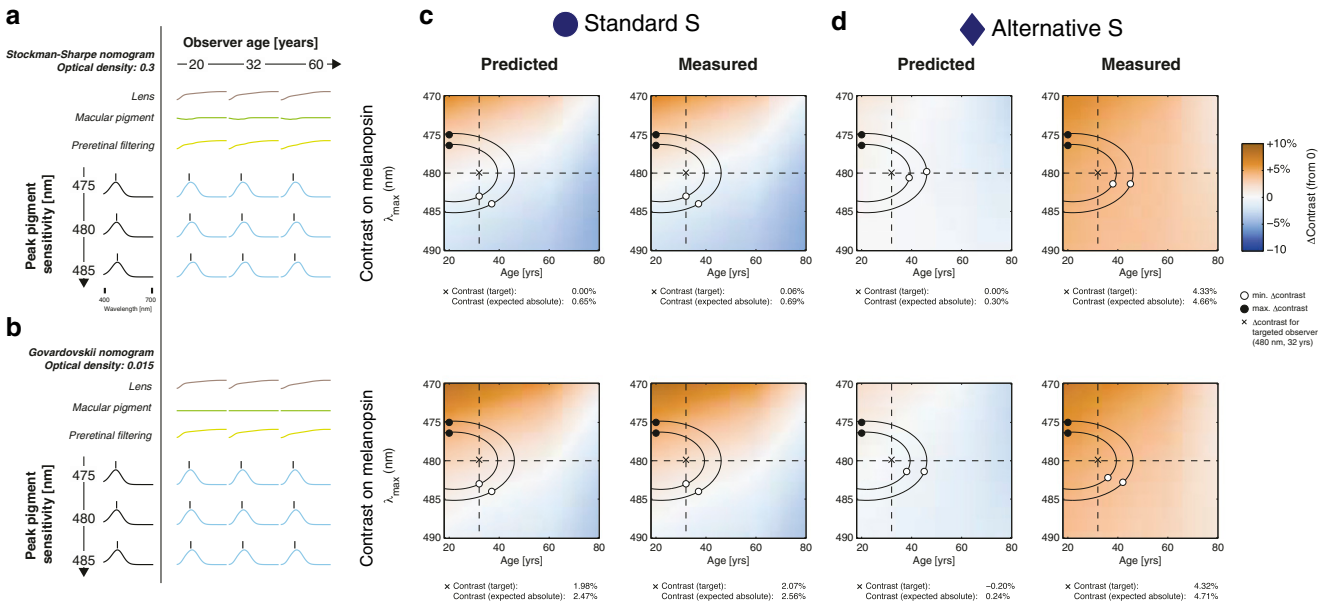

Fig. S2. Observed S opponency is not due to artifactual stimulation of melanopsin. The degree to which silent substitution is successful in isolating photoreceptor classes depends on the spectral sensitivity estimates used to calculate modulation spectra and the precision of stimulus control. To rule out negative contrast splatter of the nominally S-silencing modulation on melanopsin, which could produce an artifactual out-of-phase response in our measurements of the S-directed modulation, we explored the effect of variation in melanopsin spectral sensitivity. (*A*) Spectral sensitivity estimates of melanopsin obtained using the Stockman–Sharpe nomogram (1), a field size of 10°, adjusting for prereceptoral filtering according to the CIE standard for cone fundamentals using the observer age parameter (20–80 y) (2), and assuming a peak optical density of 0.3 (melanopsin-a). Wavelength of peak sensitivity λ_{max} was varied between 470 and 490 nm. Vertical bars above spectral sensitivity plots indicate nomogram λ_{max}. Prereceptoral filtering can shift λ_{max} of the fundamental from that of the nomogram. (*B*) Physiologically based (3) spectral sensitivity estimate of melanopsin obtained using the Govardovskii nomogram (4), a field size of 27.5°, adjusting for prereceptoral filtering according to the CIE standard for cone fundamentals using the observer age parameter (20–80 y) (2), and assuming a peak optical density of 0.015 (melanopsin-b). Wavelength of peak sensitivity λ_{max} was varied between 470 and 490 nm. (*C*) Contrast splatter of the standard S-directed modulation onto melanopsin as a function of melanopsin λ_{max} and observer age for both predicted spectra (*Left*) and spectroradiometrically measured spectra (*Right*). The upper panels are for the estimate of melanopsin spectral sensitivity in *A*; the lower panels are for the estimate of the melanopsin spectral sensitivity in *B*. Crosshairs indicate contrast for the theoretically targeted observer (melanopsin λ_{max} = 480 nm, observer age 32 y). Ellipses trace the photoreceptor contrast associated ± 2 and ± 3 SD of the expected population variation in the CIE age parameter (SD estimated as 7 y) and variation in the λ_{max} of melanopsin. Subjects 2–16 in the study had a mean (± SD) age of 21 ± 6 y, which centers the ellipse to the left of the nominal targeted age of 32 y of the observer. No measure of the variability of λ_{max} of melanopsin exists for human observers; an SD of 1.5 nm was assumed [which is the maximum of the variability estimated for the human L, M, and S cone classes (5)]. The points of maximum and minimum contrast observed within the biological variability ellipses are indicated and reported in Table S1, as is the mean absolute expectation of contrast. (*D*) Contrast splatter of the alternative S-cone modulation onto melanopsin. Same format as in *C*.

1. Stockman A, Sharpe LT (2000) The spectral sensitivities of the middle- and long-wavelength-sensitive cones derived from measurements in observers of known genotype. *Vision Res* 40(13):1711–1737.
2. CIE (2006) Fundamental chromaticity diagram with physiological axes – Part 1. Technical Report 170-1 (Central Bureau of the Commission Internationale de l'Éclairage, Vienna).
3. Brown TM, et al. (2013) The melanopic sensitivity function accounts for melanopsin-driven responses in mice under diverse lighting conditions. *PLoS ONE* 8(1):e53583.
4. Govardovskii VI, Fyhrquist N, Reuter T, Kuzmin DG, Donner K (2000) In search of the visual pigment template. *Vis Neurosci* 17(4):509–528.
5. Webster MA, MacLeod DI (1988) Factors underlying individual differences in the color matches of normal observers. *J Opt Soc Am A* 5(10):1722–1735.

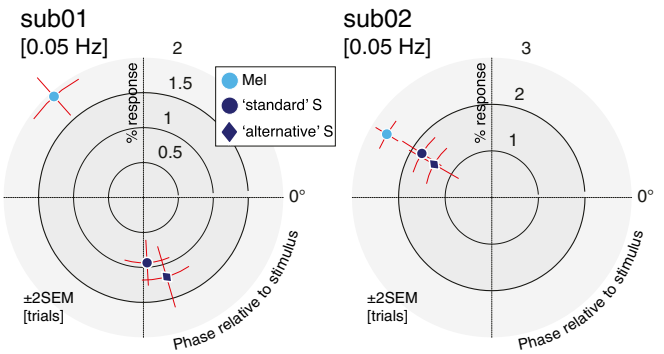

Fig. S3. Similar results obtained with standard and alternative S-directed modulations. For subjects 01 and 02, we measured responses at 0.05 Hz for both standard S-directed modulation (120-s trials) and the alternative S-directed modulation (45-s trials). Results for the two modulations are similar. Each panel shows response amplitude and phase for one subject, for the melanopsin-directed modulation and the two S-directed modulations. In this polar plot amplitude is in units of percentage of pupil diameter change, whereas phase is relative to stimulus onset.

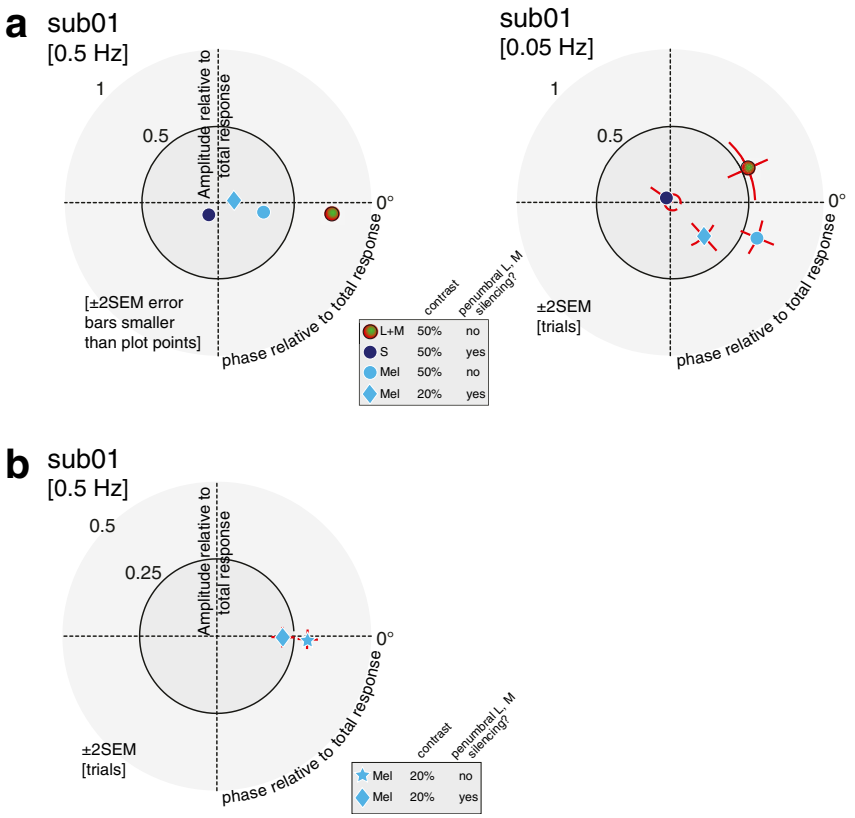

Fig. S4. Similar results obtained when silencing penumbral cones. A recent study (1) reported that four photopigment classes were required to fit human psychophysical data of detection of four primary stimuli, raising the possibility of melanopsin-mediated visual perception. This was observed to persist even when the spectral change was presented as 40-Hz flicker. The authors considered (but did not experimentally address) the possibility that this fourth photopigment class was actually L and M cones positioned in the shadow (penumbra) of retinal blood vessels, and thus subject to a hemoglobin spectral filter. Because of the minimal retinal surface subtended by penumbral cones, we consider it unlikely that the stimulation of penumbral cones would contribute substantially to the pupil response. Nonetheless, we created an S-cone-directed and melanopsin-directed modulation that also silences the predicted spectral sensitivities of penumbral cones. The maximum melanopsin contrast available for the penumbral cone silent, melanopsin-directed modulation was 20%, compared with the 50% melanopsin contrast available in the primary experiments that did not attempt to silence penumbral cones. For these control experiments, we implemented modulations tailored to the age of the subject and the field size of our experiment (27.5°) and that incorporated an estimate of fraction of pigment bleached. By the time we conducted these experiments, we had also made refinements to our stimulus control procedures (primarily better fitting of the gamma functions of our device) that led to better agreement between predicted and measured modulations. Information on estimated splatter for these experiments is provided in the legend to Fig. S5. The mean background light level used in these control experiments had a luminance of 1,566 cd/m^2, and the estimates of pigment bleaching were with respect to this value. (*A*) For subject 01, we measured the pupil response to 0.5- and 0.05-Hz stimulation with L+M- (50% contrast), S-cone-, and melanopsin-directed (50% contrast) and melanopsin-directed/penumbral cone silent (20% contrast) modulations using 45-s trials. Points are plotted relative to the complex sum of the responses to the three 50% contrast modulations (Mel, S, and L+M). The penumbral cone silent modulations produce the same form of responses recorded earlier for this subject. Appropriately, the response to the penumbral cone silent melanopsin modulation is reduced, corresponding to the decrease in available melanopsin contrast. The amplitude of pupil response to the 50% melanopsin contrast modulation at 0.5 Hz was ∼1.9% and ∼4.3% at 0.05 Hz, similar to the values obtained in the main experiments and with similar phase relations (Figs. 3 and 4). The S-cone response is similar to that obtained in the main experiments at 0.5 Hz and smaller at 0.05 Hz (but with a large SE because fewer trials were used in this control experiment). The opponent nature of the S-cone response continues to be observed in these control data. (*B*) In a second set of measurements for subject 01, we measured the pupil response to 0.5-Hz melanopsin-directed stimulation that did or did not silence the penumbral cones, with the modulations matched at 20% contrast. There was minimal difference in the amplitude or phase of the pupil response evoked by these stimuli. These results establish that penumbral cone stimulation cannot fully account either for the measured response to melanopsin-directed stimulation or for the opponent S-cone response. We note that these results do not speak generally to the role that incidental penumbral cone stimulation might play in measurement of perceptual responses to putative melanopsin-directed stimuli, where sensitivity to stimulus spatial structure might be enhanced relative to what is observed for the pupillary response.

1. Horiguchi H, Winawer J, Dougherty RF, Wandell BA (2013) Human trichromacy revisited. *Proc Natl Acad Sci USA* 110(3):E260–E269.

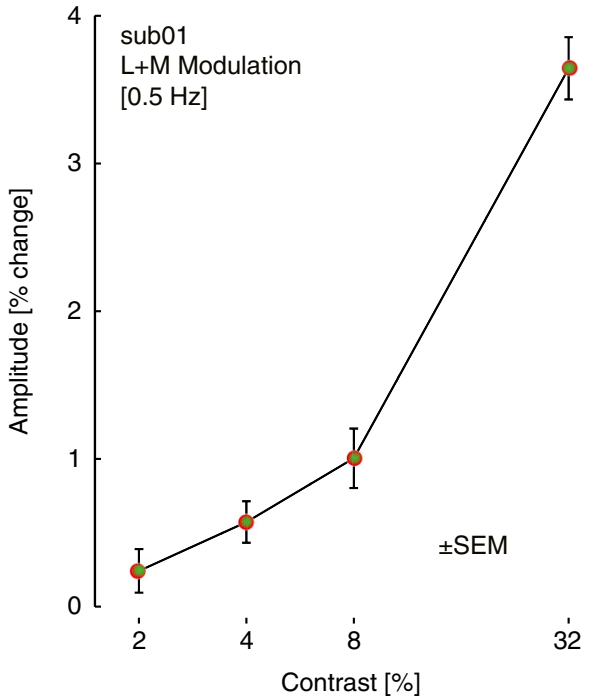

Fig. S5. L+M contrast response function. The pupil response to a 0.5-Hz modulation of L+M-directed stimulation was obtained for subject 01 at a range of contrast levels between 1% and 32% contrast. The contrast response function is notable for the absence of a compressive nonlinearity in the low-contrast regime, and in fact the observed nonlinearity is somewhat expansive. Phase was essentially uniform across contrast variation, with all responses within 0.15 π radians of the mean phase across all responses. This indicates that a small amount of inadvertent contrast on L and M cones in our nominally melanopsin stimulus is unlikely to explain the measured melanopsin responses. The response of subject 01 to the 50% melanopsin-directed stimulus at 0.5 Hz was ~1% (Fig. S4). To produce a response of this size at this stimulation frequency, the splatter of the melanopsin-directed stimulus onto the L and M cones would have to be ~8%. Taking ± 2 SD in the known variability in the λ_{max} of L and M cone (1), and the known variation in lens density and prereceptoral filtering at a given observer age (2), we calculate that the maximum splatter of the measured 50% melanopsin modulation used in these control studies onto L and M cones is 4.3% (maximum taken over the 95% confidence interval computed using the procedures described to produce the values provided in Table S1 for subject 01, but applied to the control modulations used here), and that the mean absolute expectation of splatter is 2.2%. Therefore, we consider it unlikely that inadvertent stimulation of L and M cones by our melanopsin stimulus is responsible for the responses observed from melanopsin-targeted stimulation at 0.5 Hz. At lower temporal frequencies of stimulation, where the size of the melanopsin-driven response rises with respect to that from L+M stimulation (Fig. 4 and Fig. S4), the possibility of inadvertent L+M stimulation as the source of apparent melanopsin response becomes ever less plausible.

1. Webster MA, MacLeod DI (1988) Factors underlying individual differences in the color matches of normal observers. *J Opt Soc Am A* 5(10):1722–1735.
2. Xu J, Pokorny J, Smith VC (1997) Optical density of the human lens. *J Opt Soc Am A Opt Image Sci Vis* 14(5):953–960.

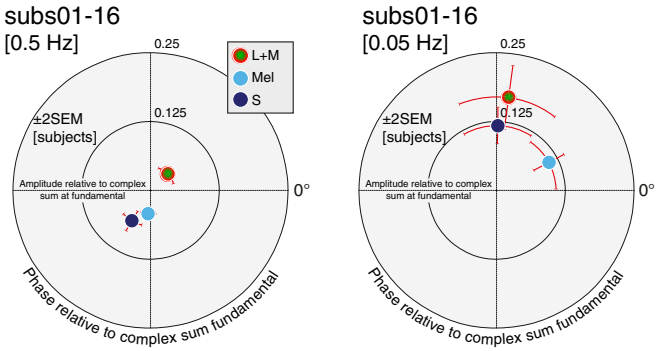

Fig. S6. Pupil responses at the second harmonic. Each panel shows the mean (over subjects) pupil response at the second harmonic of the stimulation frequency for 0.5 (*Left*) and 0.05 (*Right*) stimulation. Responses for L+M, melanopsin, and S are shown. In each panel, amplitude and phase are expressed relative to the complex sum of the response at the fundamental for these three modulation directions (the same convention as in Figs. 3 and 5).

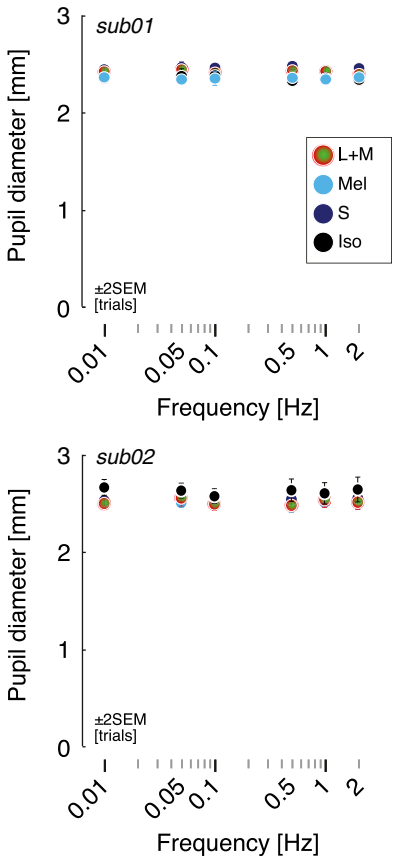

Fig. S7. Mean pupil diameter does not depend on modulation direction or frequency. Each panel shows the mean pupil diameter as a function of modulation frequency for one subject. Pupil diameter for different modulation directions is indicated by the color of the plotted points.

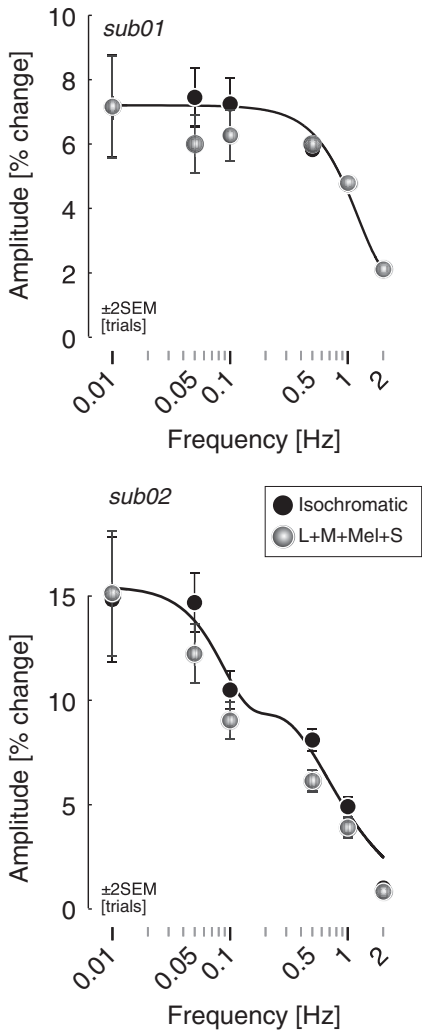

Fig. S8. Isochromatic responses are approximated by the sum of photoreceptor specific responses. Each panel compares, for one subject, the amplitude response at the fundamental measured to an isochromatic modulation—which nominally stimulates all photoreceptor classes with equal contrast and phase—and the complex sum of the responses to the L+M-, melanopsin-, and S-directed modulations. The agreement is good. The solid line is the fit of the two-filter linear model to the isochromatic modulation data, with parameters as provided in Table S2.

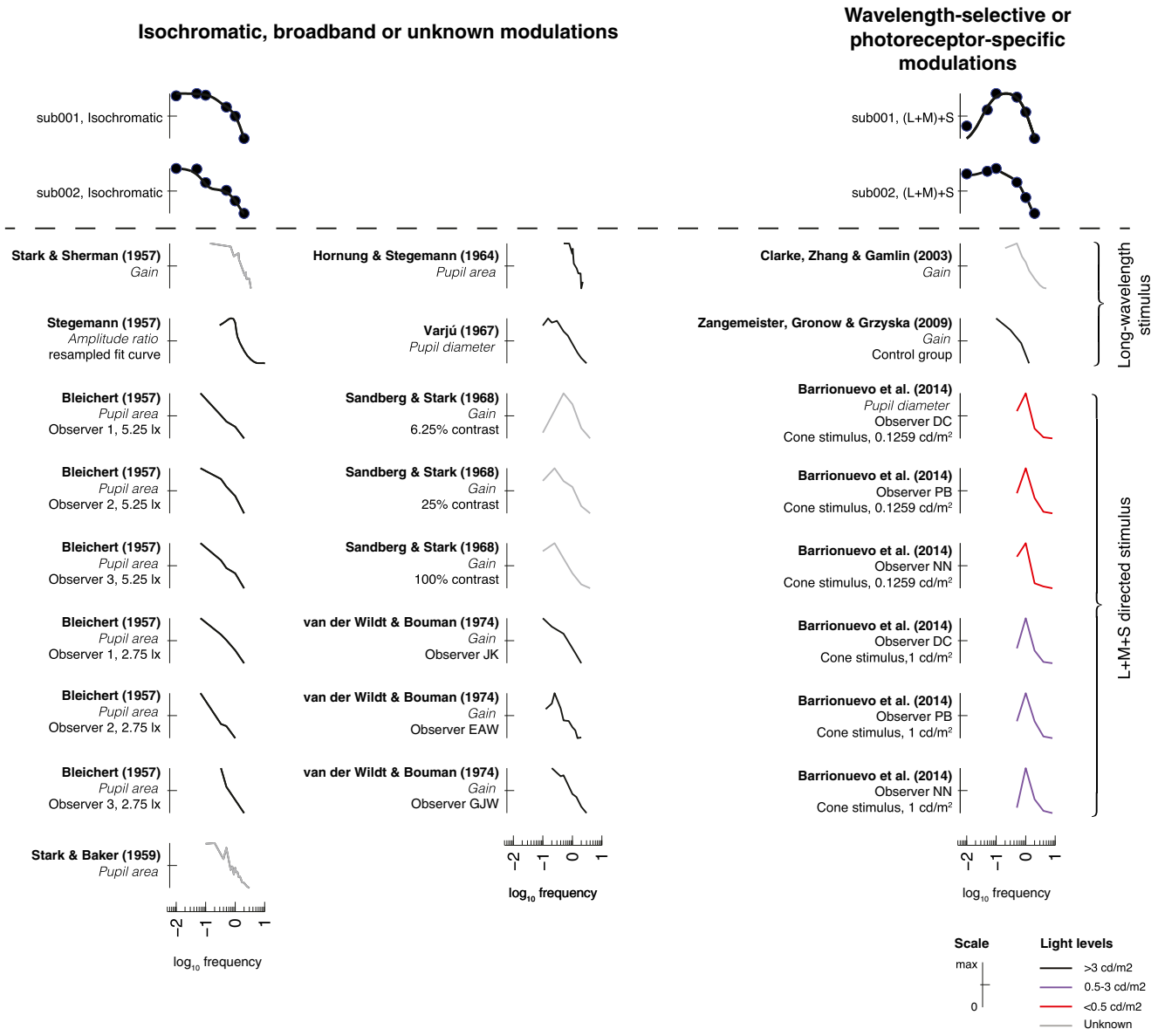

Fig. S9. Observed isochromatic and cone-driven temporal transfer functions compared with prior reports. Pupil response temporal transfer functions reported previously in the literature were extracted in tabular form or reconstructed from graphical representations when tables were not available. The function extracted from each study was normalized to its maximum response. The italicized text for each study indicates the type of measurement made, and we did not correct for differences in dependent measure (e.g., pupil diameter vs. pupil area). If reported, the mean light level of each study included was converted into candelas per square meter and color-coded by range. TTFs were reconstructed using Data Thief (http://datathief.org/) unless data were available in tabulated form (1, 2).

1. Sherman PM, Stark L (1957) A servoanalytic study of consensual pupil reflex to light. *J Neurophysiol* 20(1):17–26.
2. Zangemeister WH, Gronow T, Grzyska U (2009) Pupillary responses to single and sinusoidal light stimuli in diabetic patients. *Neurol Int* 1(1):e19.

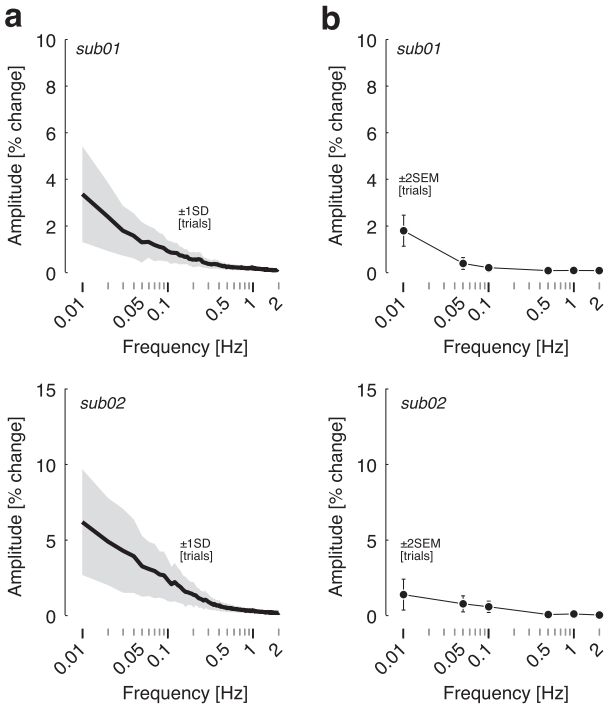

Fig. S10. Noise properties of the measures. (*A*) We obtained the average power spectrum of the residuals of the pupil measurements made during the 100-s trials for sub01 and sub02. For each trial, the amplitude of variation in pupil size at each frequency between 0.01 and 2 Hz was obtained by least-squares spectral fitting; a standard FFT could not be used because of missing time-series values in some trials (e.g., owing to blinks). Values corresponding to the frequency of the stimulus during the trial and all of its odd and even harmonics were excluded. The average of the measured amplitudes at each frequency across trials gives the power spectra shown. Intrinsic variation in pupil size over time ("pupil unrest") increases at ever lower frequencies, similar to prior reports (1). The intrinsic pupil noise inflates the variance of measurements of induced pupil response at low temporal frequencies (reflected in the error bars of Fig. 3*A*) but will not affect the expectation of the amplitude if the phase of the noise is random (or if the stimulus phase is randomized). (*B*) We considered the possibility of a phase-locked pupil response evoked by the initiation of the trial itself, independent of the stimulus modulation. Trials from sub01 and sub02 were boot-strap-sampled to measure signal amplitude at a given frequency in a set of trials that did not have stimulation at the frequency being assessed. The number of trials sampled matched the number of trials obtained for each of the plot points shown in Fig. 3*A*, and boot-strap resampling with replacement was used to obtain the SE. A small effect was seen at 0.01 Hz, indicating some phase-locking of the noise at the lowest temporal frequency. This effect approaches zero at higher frequencies. This phase-locked noise could be present in the responses measured for sub01 and sub02 at 0.01 Hz. The phase of the evoked noise is such that correction for this component of the response would slightly raise the measured response amplitudes at 0.01 Hz for melanopsin and L+M stimulation for both subjects and leave the basic shape of these TTFs little changed. For S-driven responses, correction would lower the measured amplitude for sub01, making that TTF more band-pass and raise the amplitude for sub02, making that TTF more low-pass. Overall, such a correction would little alter the general forms of the TTFs observed across these two subjects.

1. Stark L, Campbell FW, Atwood J (1958) Pupil unrest: An example of noise in a biological servomechanism. *Nature* 182(4639):857–858.

Table S1. Uncertainty in photoreceptor isolation

				Contrast, %, predicted spectra				Contrast, %, measured spectra			
Modulation direction	Receptor	Age	Nominal contrast	Target	Expected absolute	Mininum 95% [99%] CI	Maximum 95% [99%] CI	Target contrast	Expected absolute	Mininum 95% [99%] CI	Maximum 95% [99%] CI
L+M	L	21	50	53.08	52.91	52.17 [51.84]	53.51 [53.73]	57.34	57.16	56.35 [55.98]	57.81 [58.05]
		43		53.08	53.23	52.38 [51.99]	53.94 [54.18]	57.34	57.49	56.56 [56.13]	58.27 [58.52]
	M	21	50	47.38	46.78	45.10 [44.55]	48.42 [49.05]	51.31	50.68	48.88 [48.30]	52.43 [53.10]
		43		47.38	48.14	46.32 [45.57]	49.82 [51.00]	51.31	52.12	50.18 [49.38]	53.91 [55.17]
	S	21	0	2.78	3.34	1.54 [0.79]	4.98 [5.58]	3.6	4.15	2.35 [1.60]	5.78 [6.38]
		43		2.78	2.02	0.07 [-1.16]	3.95 [4.68]	3.6	2.85	0.91 [-0.30]	4.78 [5.50]
	Melanopsin-a	21	0	0	1.3	−4.16 [-5.41]	3.50 [5.12]	0.83	1.34	−3.55 [-4.87]	4.53 [6.25]
		43		0	1.43	−3.26 [-4.64]	4.94 [6.64]	0.83	1.91	−2.61 [-4.06]	6.05 [7.85]
	Melanopsin-b	21	0	−2.34	2.74	−6.19 [-7.37]	1.01 [2.56]	−1.59	2.13	−5.64 [-6.88]	1.96 [3.60]
		43		−2.34	1.99	−5.49 [-6.79]	2.26 [3.88]	−1.59	1.56	−4.90 [-6.27]	3.28 [4.99]
	Rods	21	N/A	15.09	14.44	10.20 [8.67]	18.56 [20.14]	16.93	16.23	11.71 [10.08]	20.62 [22.31]
		43		15.09	15.99	11.61 [9.95]	20.37 [21.98]	16.93	17.87	13.20 [11.43]	22.54 [24.27]
	Penumbral L	21	N/A	48.97	48.82	47.97 [47.59]	49.50 [49.74]	52.9	52.74	51.81 [51.39]	53.49 [53.75]
		43		48.97	49.09	48.13 [47.69]	49.90 [50.15]	52.9	53.02	51.96 [51.48]	53.91 [54.18]
	Penumbral M	21	N/A	43.91	43.3	40.67 [39.65]	45.54 [46.34]	47.59	46.93	44.13 [43.04]	49.32 [50.17]
		43		43.91	44.66	42.05 [40.97]	46.89 [47.89]	47.59	48.37	45.59 [44.44]	50.76 [51.82]
	Penumbral S	21	N/A	−5.11	4.63	−7.47 [-8.55]	−1.68 [-0.63]	−4	3.52	−6.44 [-7.56]	−0.50 [0.57]
		43		−5.11	5.76	−8.68 [-9.75]	−2.79 [-1.67]	−4	4.66	−7.67 [-8.78]	−1.61 [-0.47]
Melanopsin	L	21	0	−4.79	4.63	−5.22 [-5.45]	−3.87 [-3.52]	−1.73	1.54	−2.11 [-2.33]	−0.85 [-0.52]
		43		−4.79	4.93	−5.67 [-5.92]	−4.05 [-3.63]	−1.73	1.89	−2.59 [-2.90]	−1.07 [-0.67]
	M	21	0	2.81	3.43	1.52 [0.78]	5.45 [6.12]	6.83	7.49	5.47 [4.68]	9.62 [10.33]
		43		2.81	2	0.01 [-1.27]	4.11 [4.99]	6.83	5.98	3.88 [2.54]	8.22 [9.15]
	S	21	0	−6.84	8.2	−12.06 [-13.48]	−3.95 [-2.19]	−4.65	6.07	−10.11 [-11.59]	−1.62 [0.23]
		43		−6.84	4.98	−9.54 [-11.28]	−0.39 [2.68]	−4.65	2.87	−7.49 [-9.30]	2.09 [5.26]
	Melanopsin-a	21	50	50	49.88	47.77 [46.75]	51.50 [51.98]	55.88	55.75	53.60 [52.55]	57.41 [57.89]
		43		50	49.96	47.50 [46.34]	51.91 [52.49]	55.88	55.85	53.33 [52.14]	57.85 [58.43]
	Melanopsin-b	21	50	49.81	49.6	47.63 [46.71]	51.17 [51.66]	55.66	55.44	53.42 [52.49]	57.04 [57.54]
		43		49.81	49.9	47.63 [46.55]	51.78 [52.35]	55.66	55.76	53.44 [52.33]	57.69 [58.27]
	Rods	21	N/A	35.79	36.06	32.31 [30.80]	39.65 [40.92]	41.21	41.48	37.60 [36.04]	45.19 [46.49]
		43		35.79	35.33	31.24 [29.64]	39.21 [40.61]	41.21	40.74	36.51 [34.85]	44.75 [46.19]
	Penumbral L	21	N/A	1.24	1.38	0.65 [0.40]	2.30 [2.71]	4.36	4.52	3.84 [3.59]	5.38 [5.77]
		43		1.24	1.13	0.24 [-0.03]	2.18 [2.65]	4.36	4.23	3.39 [3.12]	5.21 [5.67]
	Penumbral M	21	N/A	7.49	8.16	5.51 [4.59]	11.26 [12.48]	11.58	12.27	9.45 [8.46]	15.56 [16.84]
		43		7.49	6.69	4.03 [2.98]	9.78 [11.05]	11.58	10.73	7.89 [6.80]	14.01 [15.35]
	Penumbral S	21	N/A	12.86	11.75	5.28 [2.97]	17.96 [20.33]	15.44	14.28	7.42 [4.97]	20.88 [23.40]
		43		12.86	14.33	7.81 [5.36]	20.73 [23.06]	15.44	16.99	10.07 [7.48]	23.79 [26.28]
Standard S	L	21	0	1.1	1.1	1.02 [0.97]	1.13 [1.14]	0.67	0.66	0.62 [0.58]	0.68 [0.69]
		43		1.1	1.09	0.99 [0.94]	1.15 [1.16]	0.67	0.67	0.60 [0.56]	0.70 [0.72]
	M	21	0	−0.38	0.41	−0.67 [-0.77]	−0.17 [-0.08]	−0.92	0.95	−1.20 [-1.29]	−0.71 [-0.62]
		43		−0.38	0.34	−0.61 [-0.71]	−0.08 [0.02]	−0.92	0.88	−1.15 [-1.25]	−0.63 [-0.53]
	S	21	50	51.73	51.98	50.71 [50.16]	53.10 [53.51]	52.21	52.49	51.15 [50.58]	53.67 [54.11]
		43		51.73	51.33	49.88 [49.28]	52.66 [53.10]	52.21	51.78	50.26 [49.61]	53.17 [53.64]
	Melanopsin-a	21	0	0	0.65	−1.07 [-1.60]	2.33 [3.08]	0.06	0.69	−1.06 [-1.61]	2.44 [3.20]
		43		0	0.71	−2.02 [-2.74]	1.26 [2.06]	0.06	0.7	−2.02 [-2.73]	1.36 [2.17]
	Melanopsin-b	21	0	1.98	2.47	0.85 [0.28]	4.40 [5.16]	2.07	2.56	0.89 [0.30]	4.53 [5.31]
		43		1.98	1.42	−0.17 [-0.94]	3.30 [4.12]	2.07	1.5	−0.14 [-0.91]	3.43 [4.26]
	Rods	21	N/A	−0.43	0.19	−0.70 [-0.92]	0.42 [0.63]	−0.63	0.33	−0.93 [-1.15]	0.28 [0.52]
		43		−0.43	0.78	−1.33 [-1.94]	−0.12 [0.18]	−0.63	0.99	−1.56 [-2.18]	−0.29 [0.03]
	Penumbral L	21	N/A	−0.05	0.06	−0.15 [-0.21]	−0.00 [0.01]	−0.39	0.4	−0.46 [-0.50]	−0.36 [-0.35]
		43		−0.05	0.06	−0.17 [-0.24]	0.02 [0.04]	−0.39	0.38	−0.47 [-0.52]	−0.33 [-0.31]
	Penumbral M	21	N/A	−1.44	1.49	−1.93 [-2.10]	−1.08 [-0.94]	−1.89	1.93	−2.35 [-2.52]	−1.53 [-1.39]
		43		−1.44	1.38	−1.84 [-2.03]	−0.96 [-0.82]	−1.89	1.83	−2.28 [-2.46]	−1.42 [-1.28]
	Penumbral S	21	N/A	49.95	50.35	47.28 [46.00]	53.26 [54.23]	50.01	50.42	47.33 [46.05]	53.37 [54.36]
		43		49.95	49.34	46.08 [44.76]	52.37 [53.42]	50.01	49.39	46.12 [44.80]	52.44 [53.51]
Alternative S	L	21	0	−0.17	0.16	−0.23 [-0.27]	−0.12 [-0.12]	2.07	2.09	1.96 [1.90]	2.18 [2.19]
		43		−0.17	0.18	−0.26 [-0.31]	−0.14 [-0.13]	2.07	2.03	1.90 [1.83]	2.13 [2.16]
	M	21	0	−0.81	0.78	−0.87 [-0.90]	−0.70 [-0.67]	1.88	1.93	1.84 [1.81]	1.98 [1.99]
		43		−0.81	0.82	−0.91 [-0.94]	−0.74 [-0.71]	1.88	1.84	1.76 [1.70]	1.92 [1.96]
	S	21	50	54.49	55.44	52.22 [50.86]	58.35 [59.41]	64.46	65.45	62.06 [60.63]	68.52 [69.64]
		43		54.49	53.16	49.65 [47.51]	56.58 [57.86]	64.46	63.07	59.36 [57.14]	66.68 [68.02]

Table S1. Cont.

Modulation direction	Receptor	Age	Nominal contrast	Contrast, %, predicted spectra: Target	Expected absolute	Mininum 95% [99%] CI	Maximum 95% [99%] CI	Contrast, %, measured spectra: Target contrast	Expected absolute	Mininum 95% [99%] CI	Maximum 95% [99%] CI
	Melanopsin-a	21	0	0	0.3	−0.22 [-0.41]	0.64 [0.78]	4.33	4.66	4.04 [3.82]	5.23 [5.45]
		43		0	0.33	−0.78 [-1.27]	0.22 [0.48]	4.33	3.95	3.40 [2.81]	4.64 [4.98]
	Melanopsin-b	21	0	−0.2	0.24	−0.52 [-0.76]	0.79 [1.04]	4.32	4.71	3.87 [3.58]	5.59 [5.92]
		43		−0.2	0.59	−1.19 [-1.80]	0.16 [0.52]	4.32	3.87	3.10 [2.42]	4.82 [5.27]
	Rods	21	0	0.65	0.87	0.36 [0.18]	1.33 [1.47]	4.6	4.87	4.21 [3.95]	5.50 [5.70]
		43		0.65	0.39	−0.08 [-0.43]	0.93 [1.16]	4.6	4.28	3.66 [3.23]	4.98 [5.29]
	Penumbral L	21	N/A	−0.46	0.48	−0.57 [-0.62]	−0.43 [-0.41]	1.75	1.74	1.61 [1.54]	1.82 [1.84]
		43		−0.46	0.45	−0.55 [-0.61]	−0.38 [-0.34]	1.75	1.75	1.60 [1.52]	1.84 [1.86]
	Penumbral M	21	N/A	−1.58	1.61	−1.88 [-1.97]	−1.35 [-1.24]	1.03	1.03	0.84 [0.78]	1.21 [1.29]
		43		−1.58	1.53	−1.80 [-1.91]	−1.26 [-1.16]	1.03	1.06	0.86 [0.80]	1.26 [1.33]
	Penumbral S	21	N/A	42.11	42.95	37.53 [35.38]	48.38 [50.26]	51.67	52.57	46.79 [44.50]	58.35 [60.35]
		43		42.11	40.93	35.27 [33.12]	46.46 [48.48]	51.67	50.42	44.39 [42.08]	56.31 [58.46]

Contrast splatter, that is, contrast seen by nominally silenced photopigment classes, can arise because of (*i*) uncertainty about the spectral sensitivities of the photoreceptors and their preretinal filtering and (*ii*) imprecision in stimulus production. This table reports contrast statistics for each of our modulation directions for each photoreceptor class, taken across a range of plausible biological variation in age-dependent, wavelength-specific prereceptoral filtering [via the age parameter of the CIE standard for cone fundamentals (1)] and in the wavelength of peak spectral sensitivity λ_{max} of the photopigment classes, for both predicted and measured modulations (see also Fig. S2). For L, M, and S cones, λ_{max} was assumed to be 558.9, 530.3, and 420.7 nm; for melanopsin, λ_{max} was assumed to be 480 nm. Contrast splatter is given for both predicted spectra (left) and measured spectra (right). The target contrast is provided for subject age of 32 y and with the λ_{max} values given above, which are the parameters for which the modulations used in the main experiment were designed, although here the field size is taken as 27.5°, whereas the modulations were designed for a field size of 10°. The maximum and minimum contrast was also found within the space of biological variation composed of 2 or 3 SDs in observer lens density (2) and λ_{max} of the targeted photopigment (3). Additionally, the mean absolute expectation of contrast was obtained by taking the probability weighted mean of contrast measurements within the space of lens density and λ_{max} variation. These calculations were performed separately for the mean age of subjects 02–16 (21 y) and the age of subject 01 (43 y). Contrast was calculated for two sets of melanopsin spectral sensitivity estimates (see also Fig. S2). Melanopsin-a (λ_{max} = 480 nm) was constructed using using the Stockman–Sharpe nomogram (4), a field size of 10°, adjusting for prereceptoral filtering according to the CIE standard for cone fundamentals using the observer age parameter (20–80 y) (1), and assuming a peak optical density of 0.3. Melanopsin-b (λ_{max} = 480 nm) constitutes a physiologically based (5) spectral sensitivity estimate of melanopsin, more appropriate for the stimulus conditions used, obtained using the Govardovskii nomogram (6), a field size of 27.5°, adjusting for lens transmittance according to the CIE standard for cone fundamentals using the observer age parameter (20–80 y) (7) but with filtering by the macular pigment excluded (as the central 5° of the stimulus was obscured), and assuming a peak optical density of 0.015. Importantly, the degree of splatter from the cone-directed modulations onto melanopsin yielded by the two estimates is similar. Calculated contrast upon rods and penumbral L and M cones is also presented, although there are theoretical and empirical (Figs. S1, S3, and S4) reasons to believe that these photoreceptors do not contribute to our measured pupil responses. Rod spectral sensitivity was estimated using the Govardovskii nomogram (6) by taking λ_{max} = 500 nm and peak optical density as 0.333; preretinal filtering according to the CIE standard was included. Penumbral cone sensitivity was estimated by assuming that the light seen by these cones was filtered through blood vessels of 5-μm thickness oxygenated at 85% using the spectral absorption of oxygenated and deoxygenated blood (8). Cones and penumbral cones were assumed to be affected by self-screening to an estimate of the percentage of pigment bleached by the background spectrum with a photopic luminance of 800 cd/m^2, corresponding to approximately the mean photopic luminance of the background across sessions in the main experiments. In these splatter calculations we did not systematically explore the conjoint effect of age, nominal λ_{max}, and photopigment bleaching on the splatter calculations. We separately considered the effect of photopigment bleaching in the range of 0–75% pigment bleached for L and M cones and 0–15% pigment bleached for S cones for a 21-y-old observer, with the nominal λ_{max} of each cone class. Using the melanopsin-directed modulation, we found that the effect of photopigment bleaching is on the order of a few percent at most. The range in which splatter was affected by photopigment bleaching between 0 and 75% photopigment bleached (for L and M cones) and 0 and 15% (for S cones) was 4.4, 0.5, and 0.9% for L, M, and S cones, respectively. CI, confidence interval; N/A, not applicable.

1. CIE (2006) Fundamental chromaticity diagram with physiological axes – Part 1. Technical Report 170-1 (Central Bureau of the Commission Internationale de l'Éclairage, Vienna).
2. Xu J, Pokorny J, Smith VC (1997) Optical density of the human lens. *J Opt Soc Am A Opt Image Sci Vis* 14(5):953–960.
3. Webster MA, MacLeod DI (1988) Factors underlying individual differences in the color matches of normal observers. *J Opt Soc Am A* 5(10):1722–1735.
4. Stockman A, Sharpe LT (2000) The spectral sensitivities of the middle- and long-wavelength-sensitive cones derived from measurements in observers of known genotype. *Vision Res* 40(13):1711–1737.
5. Brown TM, et al. (2013) The melanopic sensitivity function accounts for melanopsin-driven responses in mice under diverse lighting conditions. *PLoS ONE* 8(1):e53583.
6. Govardovskii VI, Fyhrquist N, Reuter T, Kuzmin DG, Donner K (2000) In search of the visual pigment template. *Vis Neurosci* 17(4):509–528.
7. Watson AB (1986) Temporal sensitivity. *Handbook of Perception and Human Performance*, eds Boff K, Kaufman L, Thomas J (Wiley, New York), Vol 1, pp 6.1–6.43.
8. Prahl S (1999) Optical absorption of hemoglobin (Oregon Medical Laser Center, Portland, OR). Available at http://omlc.ogi.edu/spectra/hemoglobin/index.html.

Table S2. Two-filter linear model

		Center				Surround			
		Amplitude	Constant	Delay	Order	Amplitude	Constant	Delay	Order
Subject	Direction	k_1	τ_1	$t_{0;1}$	n_1	k_2	τ_2	$t_{0;2}$	n_2
01	L+M	0.0381	0.2717	0.25	1	0.0139	0.5757	0.25	4
	S	−0.0061	0.2963	0.25	1	0.0050	0.4625	0.25	4
	Mel	0.0095	0.3073	0.25	1	−0.0130	1.2199	0.25	4
	Isochromatic	0.0179	0.0750	0.25	1	−0.0182	0.0750	0.25	4
02	L+M	0.0632	0.5742	0.23	1	0.0390	0.5742	0.23	4
	S	−0.0087	0.4672	0.23	1	−0.0200	1.3141	0.23	4
	Mel	0.0018	0.8340	0.23	1	−0.0390	0.8340	0.23	4
	Isochromatic	0.0562	0.3521	0.23	1	−0.0212	0.8155	0.23	4
Group (01–16)	L+M	0.0505	0.2717	0.25	1	0.0276	0.5757	0.25	4
	S	−0.0104	0.2963	0.25	1	0.0023	0.4625	0.25	4
	Mel	0.0133	0.3073	0.25	1	−0.0228	1.2199	0.25	4

Best-fitting parameters for the two-filter linear model (see *Discussion* and *SI Methods* for description of parameters).

Dataset S1. Spectral power distributions

Dataset S1

The stimulus radiance per wavelength band ($W \cdot m^{-2} \cdot sr^{-1} \cdot nm^{-1}$) of the photoreceptor directed modulations used in the main experiments. Each sheet contains the spectral power distributions for a modulation direction (L+M, melanopsin, standard S, and alternative S). Both predicted and measured background and modulation spectra are given.

Dataset S2. Individual subject measures

Dataset S2

Responses to photoreceptor-directed modulations at different temporal frequencies for each subject. Amplitude is percent change of pupil diameter. Phase is radians, with zero corresponding to an aligned constrictive response to increasing stimulus power and positive phase a constrictive response in advance of stimulus power increase.